Solid State Phenomena
ISSN: 1662-9779, Vol. 359, pp 7-11
doi:10.4028/p-veNtI2

Submitted: 2023-09-30
Revised: 2024-05-05
Accepted: 2024-05-08
Online: 2024-08-22

TEM Investigation on High Dose Al implanted 4H-SiC Epitaxial Layer

Cristiano Calabretta[1-2,a*], Nicolò Piluso[1,b], Corrado Bongiorno[2,c], Simona Boninelli[1,d], Francesco La Via[2,e], and Andrea Severino[1,f]

[1]STMicroelectronics, Stradale Primosole 50, 95121 Catania, Italy

[2]CNR-IMM, VIII Strada, 5, 95121 Catania, Italy

[a]cristiano.calabretta01@st.com, [b]nicolo.piluso@st.com, [c]corrado.bongiorno@imm.cnr.it , simona.boninelli@imm.cnr.it, francesco.lavia@imm.cnr.it, andrea.severino@st.com

Keywords: Ion implantation, Aluminum, HAADF-STEM, precipitates, EDS

Abstract. Within this work, the effect of high dose Al ion implantation on 4H-SiC epitaxial layer is displayed. Through TEM investigation it is demonstrated that the implanted surface is suitable as seed for subsequent epitaxial regrowth generating a crystal free of extended defects. In order to assess the defects within the projected range of the ion implanted area, High Angle Annular Dark Field STEM (HAADF-STEM) analyses were performed demonstrating the atomic arrangement of the lattice in correspondence of the dislocation loop and the deviation of the crystallographic planes of 4H-SiC, driven by stress relaxation, that determine the staircase configuration of the implant pattern. Further emphasis is given to the detailed analysis of the precipitates atomic structure, whose preferential localization is ascertained. Using Energy-Dispersive X-ray spectroscopy (EDS) analysis, the precipitate is finally established as Al crystal with an FCC structure.

Introduction

Post-implantation annealing in the presence of homogeneous heating of ion implanted wafer is a key process for the development of SiC-based devices [1]. The activation phase of the implanted dopant occurs following the thermal treatment where the damaged 4H-SiC lattice heals and a portion of the implanted atoms are allocated to substitutional lattice sites. It was observed that in order to recover the crystallinity, a memory of the lattice structure prior to ion implantation must exist. High resolution electron microscopy investigations have revealed that despite the 4H-SiC lattice structure is significantly strained, as implanted areas with up to 40-60% Si displaced atoms preserve the cristallinity [2]. In order to preserve lattice structure the implanted areas are annealed during ion implantation. It has also been established that the increase in the annealing temperature up to the value of the solid solubility threshold of the dopant species in the crystalline lattice of 4H-SiC induces an increase in activation. P and Al are used to achieve n-type and p-type doping. Thermal ionization energies for hexagonal and cubic sites are 60 and 120 meV, respectively, whereas for Al they are 198 and 210 meV. The reported solid solubility of the aforementioned dopant species in 4H-SiC rises with temperature, reaching 10^{20}-10^{21} cm^3 at about 2000 °C [3,4]. In this work particular attention is given to the Al implant with dopant concentrations of interest for the fabrication of 4H-SiC electronic devices demonstrating that even dopant concentrations above Al doping solid solubility limit remain suitable seed for subsequent epitaxial regrowth. A detailed pioneering investigation of the implant is provided demonstrating for the first time the presence of Al precipitates at the edges of the implant dislocation loops.

Experimental

A 6 μm epitaxial layer was grown on (0001) 4° off-axis 4H-SiC through low pressure hot wall chemical vapour deposition at 1650 °C, and doped with N at a concentration of 10^{16} at/cm^3. Al ion implantation was carried out on epitaxial layer at a temperature of 550 °C with energies between 30 and 200 keV and fluences between 3×10^{14} and 1×10^{15} cm^{-2} in order to achieve uniformly 10^{20} cm^{-3} doped box profile. A graphitic capping layer was placed on the surface to avoid the onset of step

bunching process. The sample was thus subjected to annealing at 1675 °C for 30 min to recover the implant damage and activate the Al dopant. Subsequently a further CVD growth was carried out at the temperature of 1650 °C for further 30 minutes in order to grow a 10 μm thick layer on the implanted surface. The characterization of the grown layer was carried out by μ-Raman spectroscopy. Structural investigations were performed by means of Bright Field TEM and High Angle Annular Dark Field (HAADF-STEM) analyses through ARM200F probe Cs-corrected TEM, equipped with a cold field emission gun (FEG) and operating at 200 kV with a nominal resolution of 0.68 Å.

Results and Discussion

Fig. 1a displays the image of a Brigth Field cross-sectional TEM (XTEM) acquisition of the implanted region in the epitaxial layer with characteristic defect pattern. It has been demonstrated that ion implantation under such energy range results in a region of roughly 40 nm depth unimpacted by extended defects [5] and may be used as a seed for subsequent epitaxial regrowth.

Inspection by μ-Raman spectroscopy carried out with a He–Cd laser (λ = 325 nm) and a Horiba Jovin Yvon LabRAM HR spectrofluorimeter of the regrown epitaxial layer confirmed the crystalline quality of the sample (not shown). Indeed, the TO mode from the Raman spectrum has FWHM close to the first CVD. Furthermore, epitaxial regrowth is unaffected by extended defects from the ion implanted zone, which exhibits a pattern of defects whose density depends on the concentration of Al implanted ions [6].

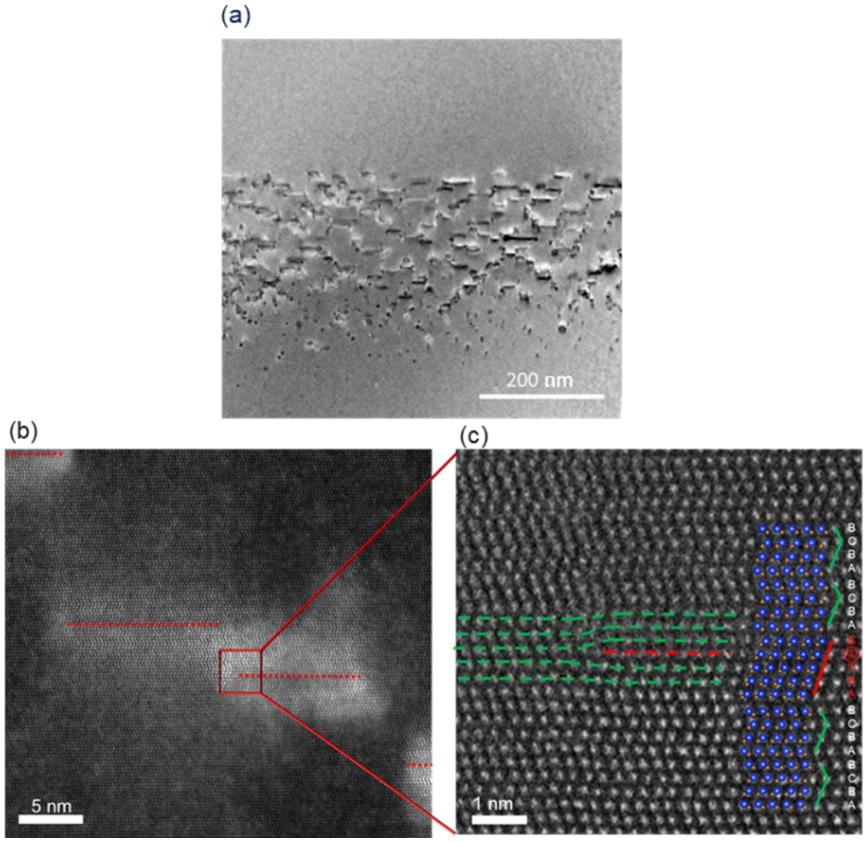

Fig. 1. Bright Field XTEM showing the implanted epitaxial layer and the subsequent epitaxial regrowth; b) MAADF-STEM acquired in the central area of the implant concerning the interaction between the different extraplanes; c) HAADF-STEM image reporting deformation of the crystal through 3C-SiC structure of the dislocation loop.

To assess the structure of the defect, ADF-STEM analysis was conducted on the sample in the projected range region. The typical arrangement of defective regions is displayed in Medium Angle Annular Dark Field (MAADF)-STEM acquisition from Fig. 1b sensible to both diffraction-based phenomena and distortions of the lattice. Each extended defect is highlighted by a red line

representing an extraplane lying in the basal plane (0001), which is surrounded by an area where the crystal is out of Bragg condition and local contrast increases due to dechanneling caused by lattice deformations. The prismatic loops move across the basal planes and merge as elastic energy diminishes, until further slips are not energetically hampered and the edges remain aligned with the c-axis as a mitigation for the strain fields developed by the dislocation loop [7]. HAADF-STEM in Fig. 1c displays the edge of the prismatic dislocation loop in greater detail. According to the description, the lattice on the left exhibits the *ABCB* stacking characteristic of 4H-SiC along the [11-20] zone axis. Indeed, the insertion of the prismatic dislocation loop implies the formation of an area of doublet elongation due to the presence the extended defect. The defect is determined by the insertion of a Si-C doublet inside the crystalline matrix revealed as an *A* layer in the stacking, indicated by red circle, and locally converting the crystal into [111] oriented 3C-SiC generated by the alignment of the sequence *ABCAB*. The high availability of Si and C interstitials due to ion implantation and annealing process results in the occurrence of dislocation loops. A high number of these pairs are accessible due to the 5.1 eV vacancy-interstitial formation energy [8]. The C interstitial migration energy of roughly 1 eV enables interstitials to move during the post-implantation annealing process. Fig. 1c, acquired in the central area of the implanted region, demonstrate how prismatic dislocation loop proceed along the crystal gathering thorough the minimization of elastic energy. Indeed, it evidences how the atomic planes deviate to relieve the stress developed as a result of the insertion of the extended defect. Moreover, Figure 2a shows the borders of the prismatic dislocation loops aligned with the c-axis, preventing defects from overlapping as a mitigation for the strain fields created by the dislocation loop [7]. With a larger field of view provided in Fig 2a, the overall effect of stress building and lattice relaxation is distinguishable. The network of dislocation loops in the implanted region was emphasized by red dashed lines on extraplanes as well as adjacent defects connection, demonstrating how the extended defects tend to compose a pattern where extraplane further expansion is hindered by the stress field of the neighboring defects, designing a *staircase* configuration driven by lattice relaxation.

Precipitates with contrast features characteristic for parallel Moire' patterns were also assessed as shown in the Bright field XTEM of Fig. 2a. HAADF-STEM investigations displayed in Fig. 2b exhibit the cubic atomic structure detail from the hexagonal perimeter region. On site 1, local EDS maps revealed a peak at 1.48 keV associated with Al, whereas 0.30 keV and 1.75 keV are connected with C and Si signals, respectively, relative to 4H-SiC present in the lamella in addition to the cluster. Region 2, on the other hand, is only sensitive to Si and C signals. Coherently with the experimentally extracted interatomic distance of 4.07 Å, these inclusions were assesed as Al precipitates incorporated within the 4H-SiC lattice.

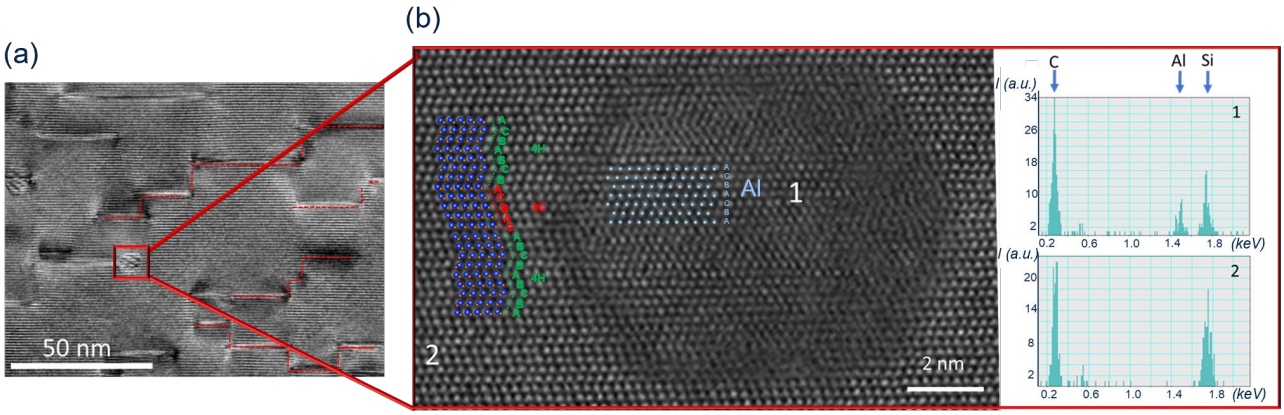

Fig. 2 a) Bright field XTEM reporting projected range dislocation loops pattern and precipitates; b) HAADF-STEM displaying Al precipitates FCC structure bounded with dislocation loop and EDS spectra from region 1 and 2.

It is clear that these structures share the presence of dislocation loop as sink regions. This behavior is motivated by the 3C-SiC inclusion characterized by a lattice parameter equal to 4.38 Å which is close to the lattice parameter of Al FCC.

Misfit dislocations flank the edge of the precipitate with the surrounding SiC crystal, indicating its accommodation in the form of relaxed crystal. The trapping of self-interstitials at the surface can lead to supersaturation of Si and C vacancies. The large atomic radius of Al relative to the host Si/C atoms and the fact that Al occupies the Si lattice in 4H-SiC, leads to diffusion of Al as typically mediated by point defects such as vacancies and self-interstitials. In particular, Al diffusion is actually a Si interstitial (Si_i)-mediated process, in which a nearby Si_i first kicks a substitutional Al atom to an interstitial site as demonstrated by Vienna ab-initio Simulation [9]. The kicked-out Al then spreads via interstitial sites. According to the migration model, the high concentration of vacancies serving as traps for interstitial atoms can result in confining Al diffusion [10]. Dislocation network would be a very effective sink for impurity atoms that are characterized by a high magnitude of $|R_{imp}-R_{hstu}|$ where R_{imp} and R_{hst} are covalent radii of the impurity and host atoms, respectively and lie within roughly a diffusion length of the dislocation network. The dopant may precipitate and become immobile if the Al concentration in this location exceeds the solubility limit. The supersaturation of the Si vacancies provides a further incorporation center for the Al atoms and stimulates the formation of aggregates particularly in the vicinity of the dislocation loops, where the conditions for lowering the solid solubility threshold are consequently established [11].

Summary

In this work it is highlighted how high dose Al implanted region is feasible as a seed for subsequent epitaxial regrowth without any propagation of extended defects from implanted area. The projected range of the implant affected by extended defects was investigated in HAADF-STEM. The atomic structure of the dislocation loop defect emerged from the analysis, consisting of a Si-C doublet inserted within the crystalline lattice and constituting a 3C-SiC inclusion. The relaxation of the crystal at the edge of the extended defects was also attested together with the staircase configuration of the pattern. The existence of precipitates just at the dislocation loop's edge was also determined and connected to the presence of 3C-SiC inclusion and to a high concentration of Si vacancies resulting in a local drop of Al solid solubility threshold.

References

[1] Nipoti, Roberta, Hussein M. Ayedh, and Bengt Gunnar Svensson. "Defects related to electrical doping of 4H-SiC by ion implantation." Materials Science in Semiconductor Processing 78 (2018): 13-21.

[2] Zhang, Yanwen, et al. "Effects of implantation temperature and ion flux on damage accumulation in Al-implanted 4H-SiC." Journal of applied physics 93.4 (2003): 1954-1960.

[3] M.K. Linnarson, U. Zimmermann, J. Wong-Leung, A. Schöner, M.S. Janson, C. Jagadish, B.G. Svensson, Appl. Surf. Sci. 203–204 (2003) 427–432.

[4] Y.A. Vodakov, E.N. Mokhov, M.G. Ramm, A.D. Roenkov, Amorphous and Crystalline silicon carbide III, Springer Proc. Phys. Vol. 56, edited by G.L. Harris, M. G. Spencer, and C.Y. Yang, (Springer, Berlin, 1992) p. 329.

[5] Severino, Andrea, et al. "Effects of thermal annealing processes in Phosphorous implanted 4H-SiC layers." Materials Science Forum. Vol. 963. Trans Tech Publications Ltd, 2019.

[6] Karlsson, L. H., et al. "Atomically resolved microscopy of ion implantation induced dislocation loops in 4H-SiC." Materials Letters 181 (2016): 325-327.

[7] Persson, PO Å., et al. "Dislocation loop evolution in ion implanted 4H–SiC." Journal of applied physics 93.11 (2003): 9395-9397.

[8] Ayedh, H. M., et al. "Elimination of carbon vacancies in 4H-SiC employing thermodynamic equilibrium conditions at moderate temperatures." Applied Physics Letters 107.25 (2015).

[9] Huang, Yuanchao, et al. "Kick-out diffusion of Al in 4H-SiC: an ab initio study." Journal of Applied Physics 132.1 (2022).

[10] Jegadheesan, V., K. Sivasankaran, and Aniruddha Konar. "Optimized substrate for improved performance of stacked nanosheet field-effect transistor." IEEE Transactions on Electron Devices 67.10 (2020): 4079-4084

[11] Usov, I. O., et al. "Transient enhanced diffusion of aluminum in SiC during high temperature ion implantation." Journal of applied physics 86.11 (1999): 6039-6042.